Desalination and Water Treatment
www.deswater.com
doi: 10.5004/dwt.2021.27367

229 (2021) 217–226
July

Evaluation of microstructured particles of egg shell and oak leaf in removal of sodium from aqueous solutions in fixed column

Akbar Rasouli[a], Ali Bafkar[b,*]

[a]*Irrigation and Drainage Engineering, Razi University, Iran, email: akbarrasouli6@gmail.com*
[b]*Assistant Professor, Water Eng. Department, Faculty of Agriculture, Razi University Kermanshah, Iran, Tel. +98 (0)9183364231; Mobile No.: +98 (0)831 8323727; Fax (Office): +98 (0)8318323727; email: bafkar@razi.ac.ir/alibafkar@yahoo.com*

Received 21 December 2020; Accepted 25 April 2021

ABSTRACT

The quantity and quality of water resources in Iran are the most important challenges in the current situation. A study of global indicators shows that if we do not pay attention to solving these problems, many fertile and residential areas will become deserted and uninhabited. On the other hand, the existence of unconventional water resources such as seas and oceans, including the Caspian Sea in the north and the Persian Gulf in the south of Iran, maybe one of the appropriate and cost-effective solutions in this regard. This study aims to investigate and compare sodium removal using a fixed column by microstructured adsorbents of oak leaf and eggshells. The results showed that the total amount of adsorption, maximum adsorption capacity and percentage of sodium removal for oak leaf and eggshell adsorbents were equal to 120.21 and 117.10 mg, 1.1 and 0.24 mg/g and 60.10, respectively. 68.88% for 5 mg/L, 194.45 and 169.93 mg, 1.77 and 0.34 mg/g, 55.56% and 54.82% for 10 mg/L and 466.83, respectively. 453.84 mg, 4.26 and 0.91 mg/g and 53.66% and 54.03% for a concentration of 30 mg/L. Fitting of continuous adsorption models on experimental data by microstructured adsorbents showed that in sodium adsorption using a fixed bed column for oak leaf and eggshell adsorbents, bed depth-service time, Thomas and Yoon–Nelson models had a better fit than the adsorption column data compared to other models. Based on the results of this study, the microstructured adsorbents of oak leaf and egg shell have a high ability to remove sodium ions.

Keywords: Sodium removal; Microparticles; Oak leaf; Egg shell; Fixed bed column

1. Introduction

In areas where freshwater is scarce, there is a growing need for low-quality water. In this regard, unconventional waters such as agricultural drains, brackish waters, brackish water and urban wastewater can be considered as valuable resources [1]. Pour Mohammad [2] investigated the effect of Conocarpus nanostructured adsorbent on the removal of cadmium from an aqueous solution by continuous and discontinuous systems. The results of continuous experiments showed that the total amount of cadmium adsorbed and the adsorption capacity of the column increased with increasing concentration of incoming cadmium in the column and the Adams–Bohart model was more consistent with the laboratory data. Farzi et al. [3] investigated the effect of nanostructured adsorbents of sugarcane straw on the removal of cadmium from an aqueous solution by continuous and discontinuous systems. The results of continuous experiments showed that increasing the concentration from 5 to 20 mg/L, the maximum adsorption capacity of cadmium ion increased from 0.91 to 2.08 mg/g and in contrast, the adsorption efficiency decreased from 48.8% to 30.32%. The results of fitting continuous models showed that Thomas and Yoon–Nelson models with a correlation coefficient above 0.95 were more consistent with laboratory data than other models Pahlavanzadeh and Zarenejad

* Corresponding author.

1944-3994/1944-3986 © 2021 Desalination Publications. All rights reserved.

Ashkazari [4] studied the de-fluoridation of drinking water with a fixed bed column using a cheap bauxite adsorbent. In this study, the continuous adsorption process was used to separate fluoride and an equilibrium concentration diagram was drawn over time. The results show continuous fluoride adsorption with both Langmuir and Freundlich models, but it is more consistent with the Langmuir model. The results of the study suggest bauxite as an effective fluoride adsorbent with efficiency in various industries. Amirnia et al. [5] investigated the removal of copper ions by a maple leaf in a renewable continuous flow column. The results showed that the adsorption percentages for metal concentrations of 15, 50 and 150 mg/L in less than 2 min were 82%, 85% and 90%, respectively. The adsorption process of Cu (II) by the adsorbent is followed the quasi-second order kinetics model (Huo et al.) and Langmuir isotherm. Copper adsorption was also affected by the adsorption mechanism.

Goli and Upadhyayula [6] studied nitrate removal from water by chitosan/alumina composite using a continuous column with a fixed bed. The results showed that the fracture curves were significantly affected by changes in flow, initial concentration, and bed depth, so that the removal efficiency, fracture time and wear decreased with increasing nitrate concentration and flow intensity and increased with increasing bed height. Thomas and Yoon–Nelson models were used for experimental experiments and the data obtained from both models were in good agreement with the experimental results. Murithi et al. [7] investigated the removal of zinc(II) ions from industrial wastewater by bone using a fixed column. The effects of bed height (2–10 cm), flow rate (5 to 10) ml per minute, and concentration (solution in the ratio of 1:1 and 1:2) on the parameters of the failure curve were determined. The highest bed capacity was 476.2 mg/g using a column height of 10 cm, a concentration of 1:2 and a flow rate of 5 mL/min. The results showed that the adsorption capacity increases with the increasing concentration of input ions and bed height and decreases with increasing current intensity. The data followed the models of Adam-Bohart, Thomas and Yoon–Nelson.

Baker and Ghanem [8] studied the behavior and separation efficiency of natural bentonite to remove sulfate from water using continuous columns and discontinuous methods. The results showed that the maximum adsorption occurred in the range of pH = 2–3 and the contact time was 60 min. The adsorption process followed the quasi-second order kinetics model (Huo et al.) and the Langmuir isotherm. A positive value of ΔH (15.2 kJ/mol) indicates that the adsorption of sulfate ions on the adsorbent is an endothermic process and a positive value of ΔS (22.1 J/mol K) indicates that the adsorption with a small amount of positive energy (ΔG) is optimally done [8]. Ovary skin membrane is a waste product that is obtained in large quantities from the food industry. The main constituents of the membrane are protein and calcium. In addition to these organic compounds, other mineral compounds such as sulfur, silica, zinc, etc. are present in the membrane [9]. Oak leaf also contain the main constituents of silica and calcium, as a result of which these elements can be exchanged with polluting ions during the ion exchange reaction. The aim of this study was to investigate the fracture curves of the column bed for the removal of sodium from aqueous solutions using oak leaf and eggshell adsorbents. Also, the effect of sodium concentration in the form of their fracture curves is investigated.

2. Materials and methods

2.1. Continuous adsorption experiments

Research in the field of solid–liquid adsorption technology is performed in the form of equilibrium discontinuous adsorption experiments and dynamic continuous flow adsorption studies. Evaluation of equilibrium adsorption performance should be complemented by directional kinetic studies and finally, dynamic continuous flow experiments [10]. In continuous input currents, the equilibrium region gradually moves down the column. As the equilibrium region reaches the lower end of the column bed, the concentration at the output increases and eventually equals the input concentration. The point at which the output concentration increases rapidly is called the breakpoint (break time). Fracture and burnout points are points where the ratio of output concentration to input concentration is 5% and 95%, respectively [11]. The efficiency of an adsorption column is described by the refractive index, which indicates the adsorption behavior (sodium) during removal from the containing solution along the column bed and is generally normalized as the output-to-input concentration ratio per unit time or output volume, which is defined for a specific context [12]. The volume of the output fluid can be obtained from the following equation:

$$V_{\text{eff}} = tQ \tag{1}$$

where Q and t are the volume flow in milliliters per minute (mL/min) and the total flow time in minutes (min), respectively.

The area under the refractive curve (A) can be calculated by integrating the adsorbed sodium concentration curve (Na_{ad}) versus time (t) and it can be used to calculate the total amount of adsorbed metal (q_{total}) in the column for input and flow rates.

$$q_{\text{total}} = \frac{QA}{1{,}000} = \frac{Q}{1{,}000}\int_{t=0}^{t=\text{total}} \text{Na}_{\text{ad}}\,dt \tag{2}$$

The total amount of metal ions entering the column (m_{total}) and the percentage of total removal (%) can be calculated from Eqs. (3) and (4), respectively [13]:

$$m_{\text{total}} = \frac{C_0 Q t_{\text{total}}}{1{,}000} \tag{3}$$

$$\text{Total Removal}(\%) = \frac{q_{\text{total}}}{m_{\text{total}}} \times 100 \tag{4}$$

The adsorption capacity of the column (q_{eq}) can be calculated using Eq. (5) as the total amount of ions adsorbed at the end of the total flow time (q_{total}) in the adsorbent mass unit (X) [12]:

$$q_{eq} = \frac{q_{total}}{X} \quad (5)$$

The residence time in the empty bed (EBRT) represents the time required to fill the empty column with the solution in minutes, which can be calculated from Eq. (6) [14]:

$$EBRT = \frac{V}{Q_{in}} \quad (6)$$

The volume of the bed is in milliliters (mL) and the flow rate to the column is in milliliters per minute (mL/min). For continuous experiments, a pilot as shown in Fig. 1 was used.

At this stage of the experiments, a fixed bed adsorption column was used to investigate the adsorption process on a larger scale. For experiments, a fixed-bed glass column (inner diameter 3.4 cm and height 84 cm) and a flow inlet flow of 50 mL/min were used. At the bottom of the adsorption bed, a glass filter with a pore diameter of 400 μm was placed to prevent the adsorption of fine particles. Above the adsorbent, fiberglass was used to evenly distribute the inlet solution to the column over the entire surface of the adsorbent. The adsorbent used in the continuous experiments had an approximate size of 500 μm, and sieves No. 20 (with a pore diameter of 841 μm) and 40 (with a pore diameter of 420 μm) were used to achieve this size and the remaining adsorbent was collected on sieve No. 40. The sodium solution was fed to the system at a pH of 5 and concentrations of 5, 10, and 30 mg/L at laboratory temperature (20°C ± 2°C) by gravity flow. The pump used to power the system was a peristaltic pump [15]. The adsorbent was first mixed with double distilled water and poured into a test column. Then, using a peristaltic pump, a flow rate of 50 ml/min entered the column. After passing through the adsorbent bed, it came out of the two valves installed at the bottom of the column and samples were prepared from this part at different times. After launching the pilot and passing the solution through the column, sampling of the column at times of zero (the first output from the column), 5, 15, 30, 45, 60, 120, 180 min, etc., input concentration and cessation of sodium metal uptake were performed until the output concentration is balanced [16]. The sampling time of each column varies depending on the type of adsorbent, adsorption rate, adsorbent concentration, ambient pH, etc. Therefore, for different adsorbents under the same conditions, this time is different.

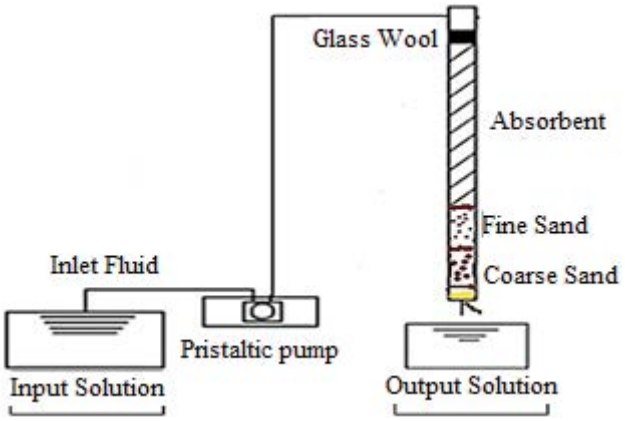

Fig. 1. Schematic of the laboratory column used in continuous experiments.

In continuous experiments, changes in sodium output concentration with time were studied for the studied adsorbents in micro size at a flow rate of 50 mL/min and concentrations of 5, 10 and 30 mg/L in synthetic solution. Sodium concentration of the samples was measured by a flame photometer (model 405 G).

2.2. Continuous adsorption models

To predict the refractive index behavior of the adsorbent (sodium) in the fixed bed columns, the refractive curve models presented in Table 1 and the parameters of these models in Table 2 were used.

3. Discussion and results

3.1. Results of physical properties of nanostructured adsorbents studied

The physical properties of the adsorbents studied in this study are calculated using conventional methods and are presented in Table 3. The specific surface area is one of the important properties of the adsorbent, the higher its value, the higher the efficiency and speed of adsorption. Solubility in adsorbent water was determined using the ASTM method (D5029–98) [19]. Microstructured oak leaf adsorbent had higher water solubility (14.5%) than eggshell. The values of apparent specific gravity obtained from the studied adsorbents show that the adsorbent of oak leaf and egg shell had less and more specific

Table 1
Equations of models used in research

Model name	Nonlinear equation
Adams–Bohart	$\ln\left(\frac{C_t}{C_0}\right) = K_{AB}C_0 t - \frac{K_{AB}N_0 Z}{U_0}$
Thomas [17]	$\ln\left(\frac{C_0}{C_t} - 1\right) = \frac{K_{Th}q_0 m}{Q} - K_{Th}C_0 t$
Yoon–Nelson [18]	$\ln\left(\frac{C_t}{C_0 - C_t}\right) = K_{YN}t - \tau K_{YN}$
Dose-response model	$\frac{C_t}{C_0} = 1 - \frac{1}{1 + \left(\frac{C_0 Q_t}{q_0 X}\right)^a}$
Bed depth-service time	$\frac{C_t}{C_0} = \frac{1}{1 + \exp\left[K_{BDST}C_0\left(\frac{N_0}{C_0 U_0}Z - t\right)\right]}$

specific gravity than water, respectively, which indicates the high porosity and lightness of oak leaf adsorbent. Moisture content was obtained using ASTM method (D2867–99) [20]. The results showed that the sorbents of oak leaf and eggshells have the highest and lowest moisture, respectively.

Table 2
Definition of abbreviations used in equations used

Parameter	Definition
K_{AB}	Adams–Bohart kinetics constant (L/mg min)
N_0	Maximum volume adsorption capacity (mg/L)
Z	Depth of column bed (cm)
U_0	Linear velocity (cm/min)
C_0	Input concentration (mg/L)
C_t	Output concentration (mg/L)
K_{Th}	Thomas speed constant (L/g min)
Q	Flow rate (mL/min)
q_0	Maximum adsorption capacity (mg/g)
M	Dry adsorbent mass (g)
T	Time (min)
K_{YN}	Yoon–Nelson constant (1/min)
T	Time required for 50% adsorbent breakthrough (min)
A	Kinetics constant (dimensionless)
K_{BDST}	Constant bed depth kinetics-service time (L/mg min)

3.2. Results of qualitative analysis of elements in the microstructured adsorbents studied

Fig. 2 shows the results of the qualitative analysis of the studied adsorbents using IDEX analysis. According to the desired forms, oak leaf adsorbent has the main chemical elements of potassium, calcium, silicon, copper, and zinc and the structure of the eggshell adsorbent has the main chemical elements of calcium and copper. Silicon is the most abundant organic matter for oak leaf and calcium is the most abundant mineral for eggshells. Since the studied adsorbents do not contain the gold element, the gold element in the analysis is related to the gold coating placed on the samples.

3.3. Investigation of the infrared spectrum of adsorbents studied

Fig. 3a shows the IR spectrum of oak leaf sorbents before adsorption. The bonded vibrational frequencies are as follows: peak in wave number 3,384.43 cm^{-1} related to symmetrical tensile vibrations of hydrogen ions OH···OH, wave frequency 2,925.13 cm^{-1} related to tensile C–H bond, wavelength 1,737.1651–11.65 cm^{-1} related to The bond C=O tensile and the absorption peak 1,044.15 cm^{-1} is related to the CO bond.

Table 3
Physical properties of the adsorbents studied

Absorbent type (microstructure)	Moisture (%)	Bulk density (g/cm^3)	Solubility in water (%)	Specific area (m^2/g)
Oak leaf	5.338	0.302	14.5	259.37
Egg shell	1.20	1.37	1.6	192.90

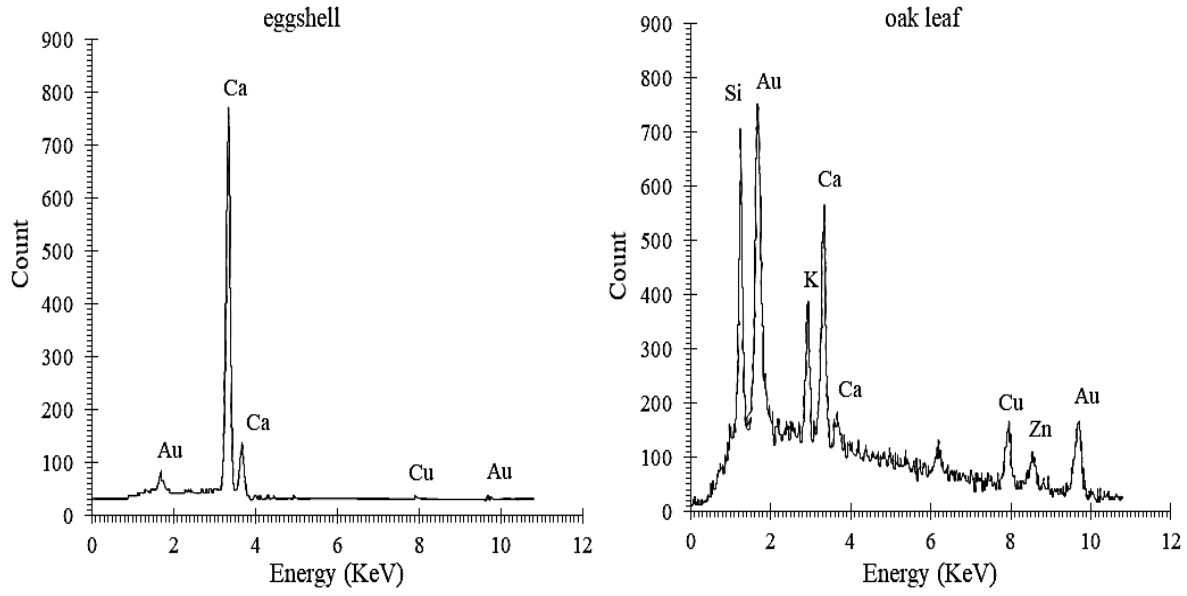

Fig. 2. IDEX image of the sample of studied attractions.

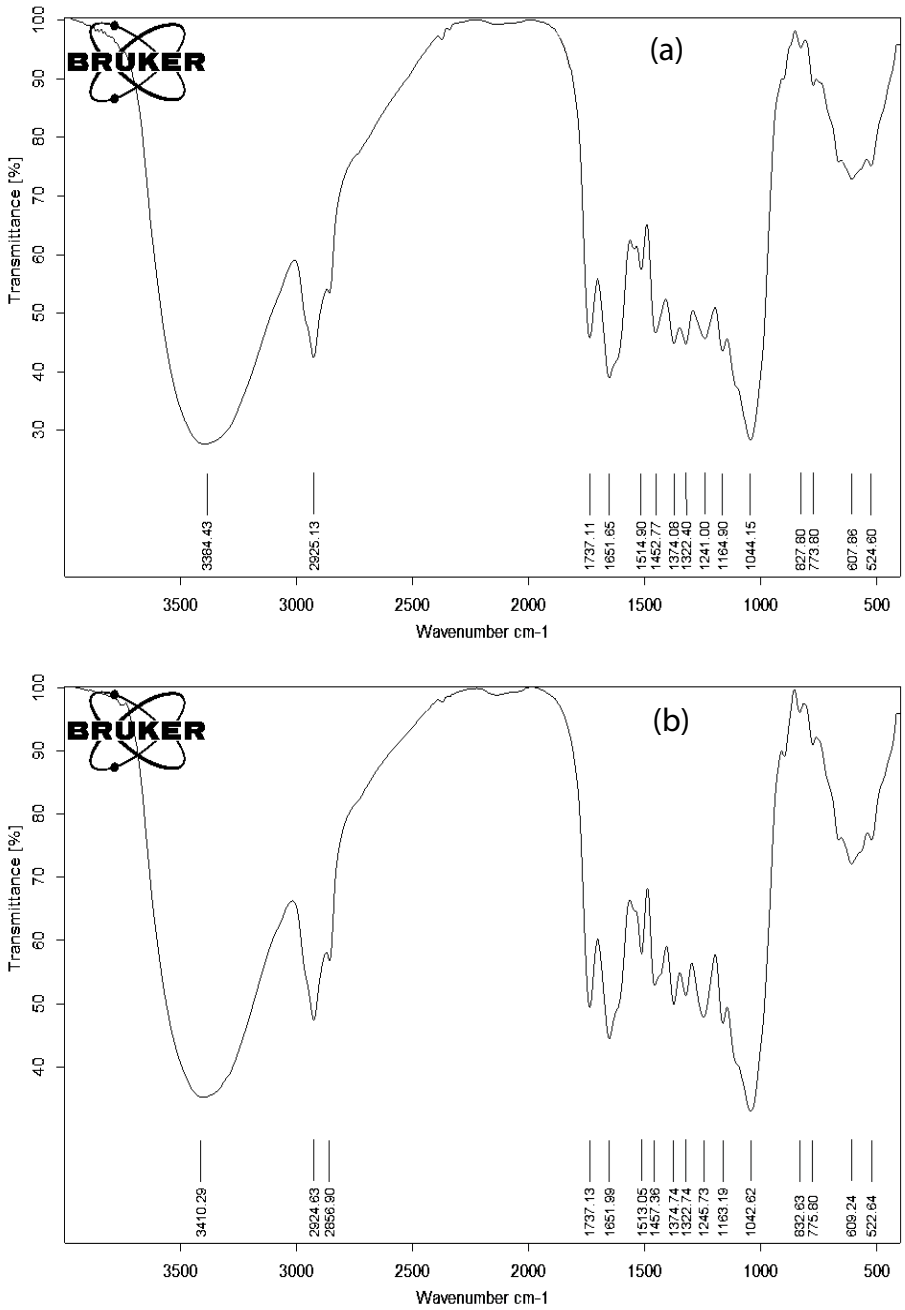

Fig. 3. Infrared spectrum of oak leaf microstructure (a) pure and (b) loaded with sodium ion.

Fig. 3b shows the IR spectra of the adsorbent oak leaf loaded with sodium ions. The bonded vibrational frequencies are as follows: wave frequency 3,410.29 cm^{-1} related to symmetric tensile vibrations of hydrogen ions OH···OH, wavelength 2,924.63 cm^{-1} related to tensile vibrations of C–H bond (group of alkanes), wavelength 1,737.1651–13.99 cm^{-1}. It is related to the tensile vibrations of the C=O bond (ester and amide group) and the absorption peak of 1,042.62 cm^{-1} is related to the C–O bond (ester group).

Fig. 4a shows the IR spectrum of the eggshell adsorbent before adsorption. The bonded vibrational frequencies are as follows: wavelength 3,329.24 cm^{-1} related to the average absorption of symmetric tensile vibrations of hydrogen bonds OH···OH, wavelength 2,875.55–2,971.71 cm^{-1} related to the tensile vibrations of C–H bond (group of alkanes) and peak absorption 1,083.13 cm^{-1} is related to C–O bond (group of esters).

Fig. 4b shows the IR spectra of the adsorbed egg shell loaded with sodium ions. The bonded vibrational frequencies are as follows: wave frequency 3,296.40 cm^{-1} related to symmetric tensile vibrations of OH···OH hydrogen bonds, wavelength 2,874.70–2,966.89 cm^{-1} related to tensile vibrations of C–H bond (alkanes) and strong absorption peak 1,083.23 cm^{-1} is related to CO bond (group of esters).

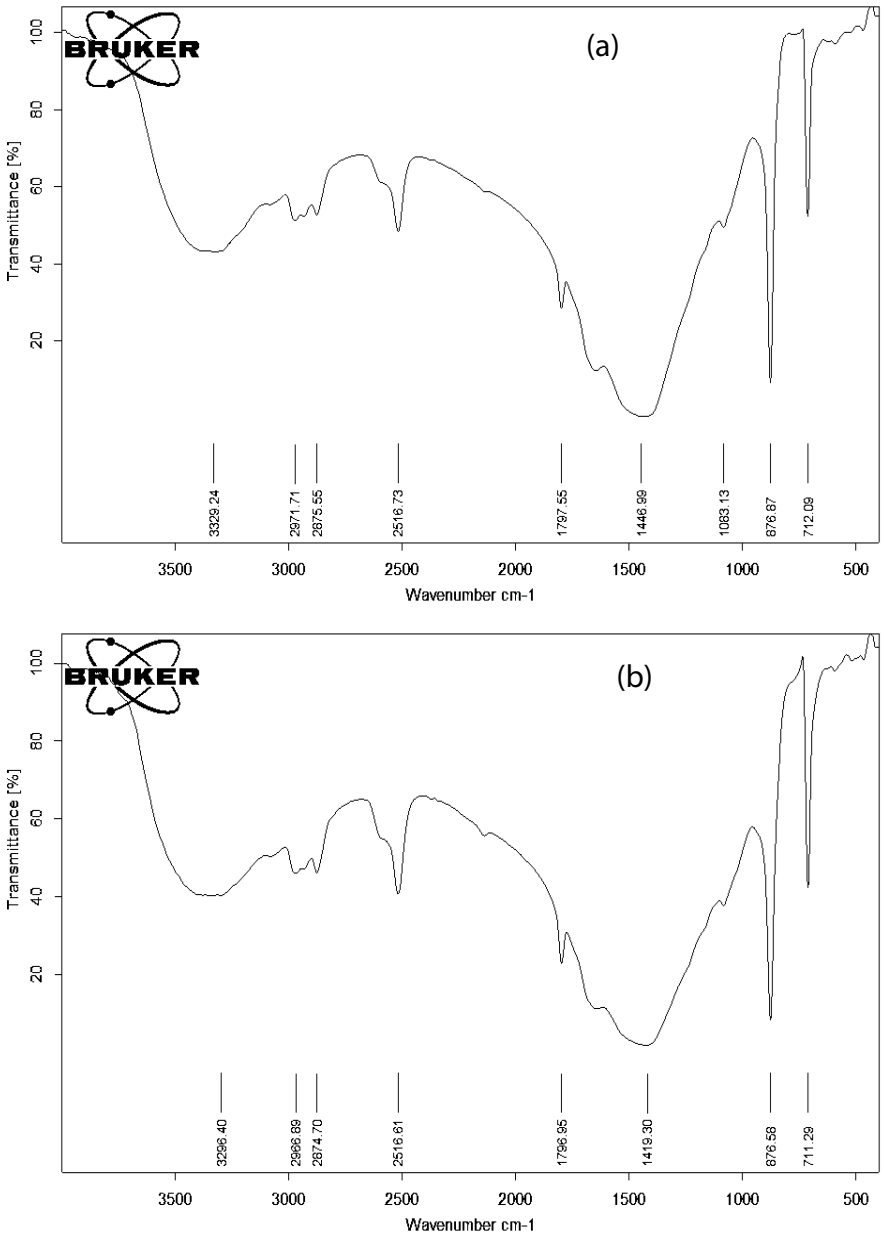

Fig. 4. Infrared spectrum of nanostructured egg shell (a) pure and (b) loaded with sodium ion.

3.4. Results of continuous tests

3.4.1. Effect of input sodium solution concentration on the column

In order to achieve the optimal performance of the DC column, the initial concentration of input sodium was changed in the range of 5, 10 and 30 mg/L. The effect of inlet concentration of adsorbent on the bed height of 40 cm and the flow rate of 50 mL/min by the refractive index for the studied adsorbents is shown in Fig. 5.

According to Fig. 5, it can be seen that by increasing the inlet concentration from 5 to 30 mg/L, the volume of adsorbent that enters the column increases and causes more metal ions to be adsorbed on the adsorption sites, resulting in faster saturation of the adsorbent and reduced failure time. Also, with increasing the input concentration of these curves, the slope increases and the failure volume decreases due to the reduction of mass transfer load between the solution and the adsorbent surface and the reduction of the driving force [21–23]. At higher concentrations, the availability of metal molecules for higher adsorption sites increases, which increases the adsorption capacity at higher concentrations, resulting in shorter breakdown times than for shorter concentrations [6]. The driving force in the adsorption phenomenon is the concentration difference between the sodium ions present in the solution and on the adsorbent surface [12]. As a result, the high driving force due to the high concentration of metal ions is an important factor in better column performance.

The effect of initial sodium concentration on the effective parameters of adsorption, such as the total amount of adsorption, maximum adsorption capacity, and the percentage of sodium removal according to the input flow rate for the studied adsorbents, are shown in Table (4). In general, the total amount of adsorption, maximum adsorption capacity, and sodium removal percentage for oak leaf and egg yolk sorbents obtained were 120.21 and 117.10 mg, 1.1 and 0.24 mg/g, respectively, and 60.10% and 68.88% for concentrations of 5 mg/L, 194.45 and 169.93 mg, 1.77 and 0.34 mg/g, 55.56% and 54.82% for the concentrations of 10 mg/L, 466.83 and 453.84, 4.26 and 0.91 mg/g and 53.66% and 54.03% for concentrations of 30 mg/L. The results of continuous experiments showed that the total amount of sodium absorbed and the adsorption capacity of the column increased with increasing concentration of sodium entering the column.

Table 4 shows that the highest adsorption rate and maximum sodium adsorption capacity are obtained at the highest metal concentration (30 mg/L), also, with increasing the concentration of the input solution, the concentration of unabsorbed ions increases, which causes the adsorption sites to be occupied and the adsorbent in the column to saturate faster when a higher concentration solution enters. According to the results, it was observed that with increasing the concentration of input sodium, the adsorption capacity increased, which was probably due to the concentration gradient and propulsion force that increased the adsorption process but quickly filled all adsorption sites. Thus, the percentage of total sodium removed as been reduced. Similar results have been obtained in the removal of cadmium from the aqueous medium using Lufa natural adsorbent [21], the removal of nitrate from water using chitosan/alumina composite using a continuous column with a fixed bed [6]; removal of zinc ions (II) from industrial wastewater by bone using a fixed column [7]; study of the fixed-bed column and modeling of adsorption of cadmium and lead by a calcareous skeleton [24] and adsorption of methylene blue on zeolite in the column with fixed bed [25].

3.5. Fitting continuous adsorption models

In this part of the study, the dynamic behavior of sodium adsorption by the studied adsorbents was investigated

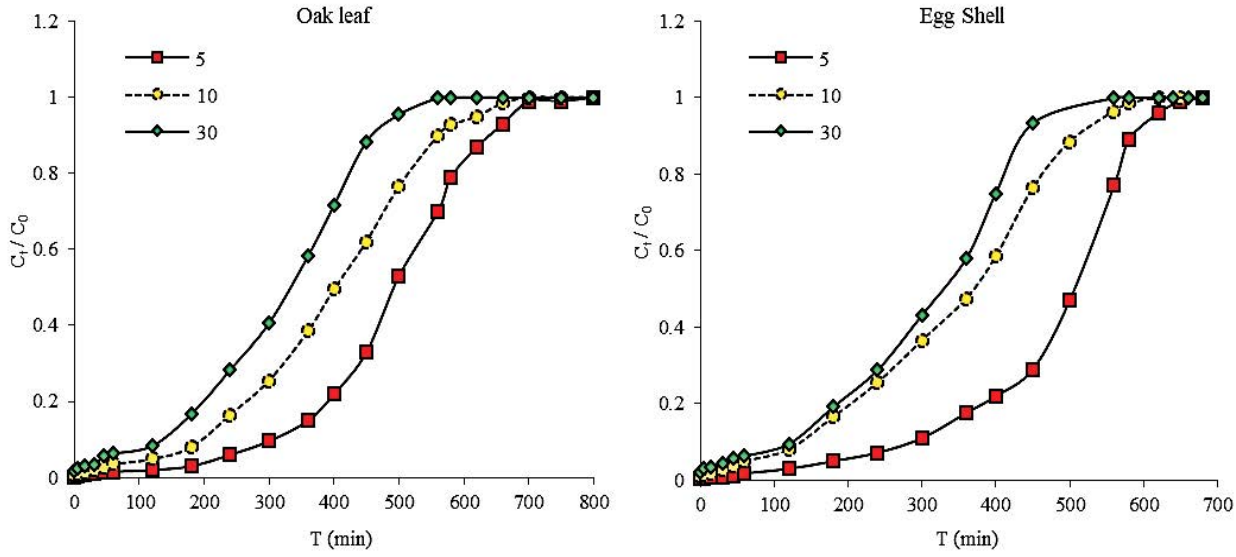

Fig. 5. Breakthrough curve of sodium removal by microstructured adsorbents studied at different concentrations (flow rate 50 mL/min).

Table 4
Effect of changes in initial concentration of sodium solution entering the column on effective adsorption parameters

Adsorbent	Column adsorption capacity (mg/g)	Total amount of adsorption (mg)	Total sodium enters the column (mg)	Total flow time (min)	Input sodium concentration (mg/L)	Flow rate (mL/min)	Total removal percentage (%)
Oak leaf	1.10	120.21	200	800	5	50	60.10
	1.77	194.45	350	700	10	50	55.56
	4.26	466.83	870	580	30	50	53.66
Egg shell	0.24	117.10	170	680	5	50	68.88
	0.34	169.93	310	620	10	50	54.82
	0.91	453.84	840	560	30	50	54.03

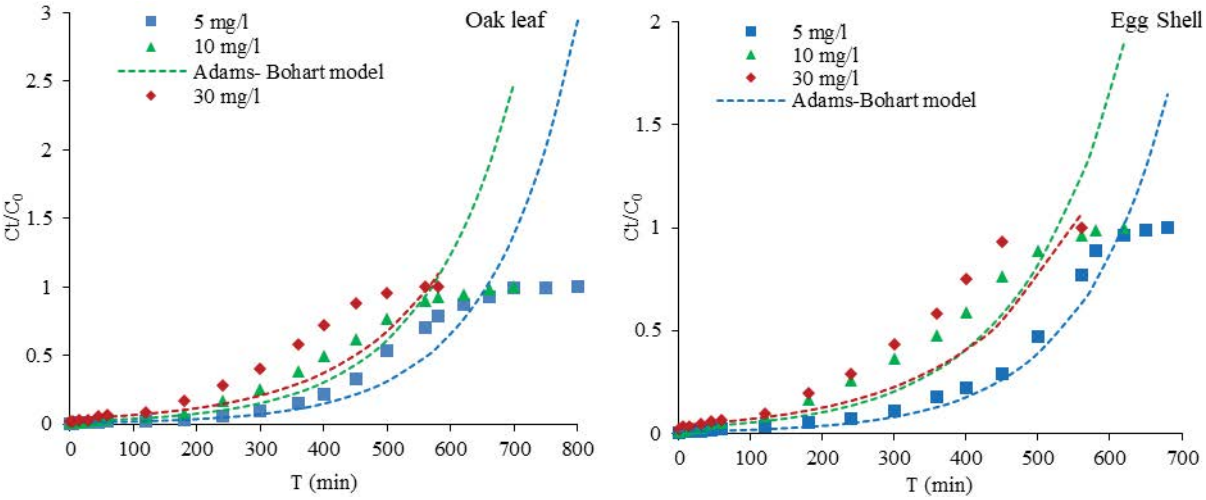

Fig. 6. Adaptation of the Adams–Bohart model to observational data at different concentrations (bed height 40 cm and flow rate 50 mL/min).

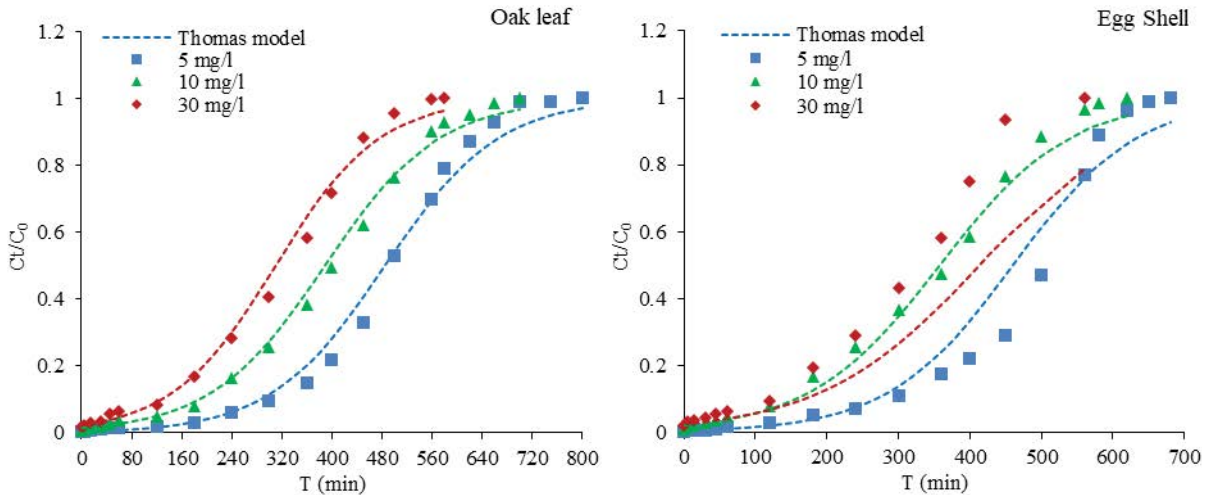

Fig. 7. Fitting of Thomas model on observational data at different concentrations (bed height 40 cm and flow rate 50 mL/min).

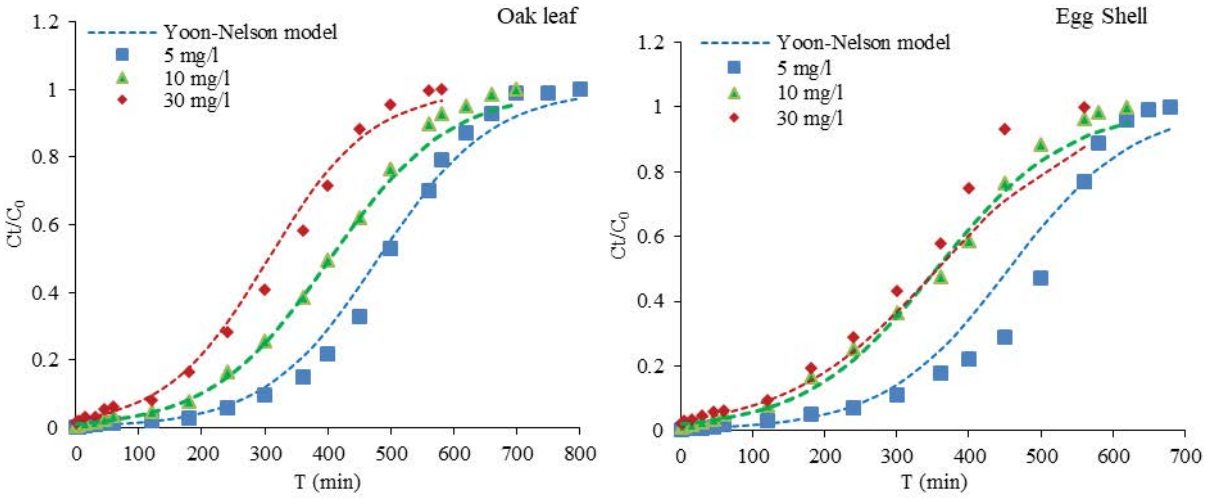

Fig. 8. Fit of Yoon–Nelson model to observational data at different concentrations (bed height 40 cm and flow rate 50 mL/min).

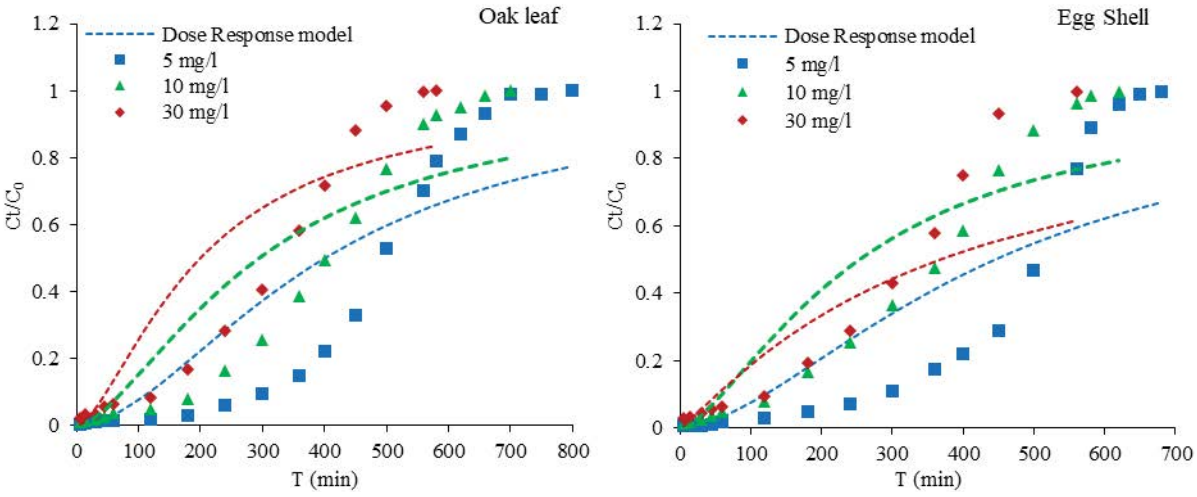

Fig. 9. Fitting of Dose-response model on observational data at different concentrations (bed height 40 cm and flow rate 50 mL/min).

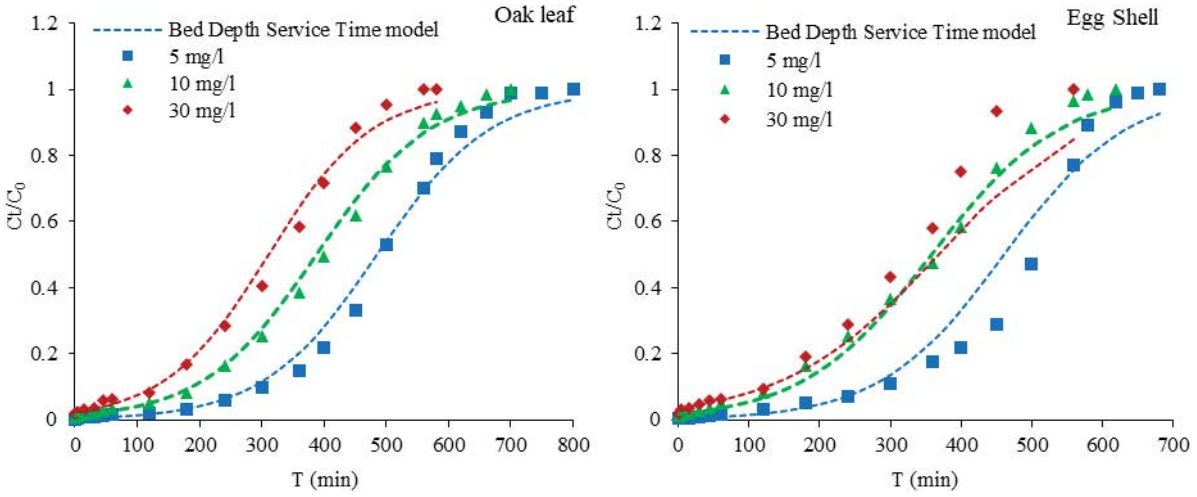

Fig. 10. Fitting of bed depth-service time model on observational data at different concentrations (bed height 40 cm and flow rate 50 mL/min).

using Adams–Bohart, Thomas Yoon–Nelson models, dose response and bed depth-service time.

Figs. 6 to 10 show the fit of continuous adsorption models to observational data at different concentrations.

According to the presented figures, it can be concluded that for oak leaf and eggshell adsorption, bed depth-service time, Thomas and Yoon–Nelson models have a better fit than the data due to having higher R^2 values and lower RMSE than other models. Figs. 7, 8 and 10 also show this appropriate fit and acceptable agreement between the observational data and the fitted theoretical lines based on these models at all sodium concentrations. Similar results were obtained in the removal of cadmium from the aqueous medium using the natural adsorbent of Lufa by the method of discontinuous and continuous equilibrium experiments [21]; nitrate removal from water using chitosan/alumina composite using a fixed bed continuous column [6]; removal of zinc ions (II) from industrial wastewater by bone using a fixed column [7]; phosphate uptake from aqueous and wastewater solutions using ocarlod zirconium (ZLO) [26]; continuous adsorption modeling for the removal of cadmium and lead ions in aqueous solution by dead calcareous skeletons [24]; removal of heavy metals using Maxima bark, salted fruit bark and sugarcane bagasse in a fixed bed column [27] and adsorption and desorption of cadmium in a fixed bed column using sunflower seed waste [16]. Among them, Thomas and Yoon–Nelson models showed a better fit of the adsorption column data than the other models

4. Conclusion

The results of continuous experiments showed that the total amount of sodium absorbed and the adsorption capacity of the column increased with increasing concentration of sodium entering the column. Fitting of continuous adsorption models on experimental data by microstructured adsorbents showed that in sodium adsorption using a fixed bed column for oak leaf and eggshell adsorbents,

the bed depth-service time, Thomas and Yoon–Nelson models were higher than the other models, respectively. They had a better fit than the adsorption column data. Based on the results of this study, the microstructured adsorbents studied had the ability to remove sodium ions.

References

[1] H. Kahrizi, Removal of Heavy Metals using Nanotechnology, Master Thesis in Irrigation and Drainage, Razi University of Kermanshah, 2015.

[2] P. Pour Mohammad, Investigation of the Effect of Conocarpus Nanostructured Adsorbent on Cadmium Removal from Aqueous Solution by Continuous and Discontinuous Systems, Master Thesis in Irrigation and Drainage, Razi University, Kermansha, 2016.

[3] S. Farzi, Investigation of the Effect of Nanostructured Adsorbent of Rice Straw on the Removal of Cadmium from Aqueous Solution by Continuous and Discontinuous Systems, Master Thesis in Irrigation and Drainage, Razi University of Kermanshah, 2016.

[4] H. Pahlavanzadeh, H. Zarenejad Ashkazari, Fluoridation of drinking water with a fixed bed column using a cheap bauxite adsorbent, Iran. J. Chem. Chem. Eng., 32 (2013) 17–24.

[5] S. Amirnia, M.B. Ray, A. Margaritis, Copper ion removal by *Acer saccharum* leaf in a regenerable continuous-flow column, Chem. Eng. J., 287 (2016) 755–764.

[6] W.M. Golie, S. Upadhyayula, Continuous fixed-bed column study for the removal of nitrate from water using chitosan/alumina composite, J. Water Process. Eng., 12 (2016) 58–65.

[7] G. Murithi, K.S. Warui, W. Muthengia, Fixed column study for the removal of zinc(II) ions from waste water by bone char rice husks ash and water hyacinth composite-mixture, Int. J. Sci. Res., 5 (2016) 708–714.

[8] H.M. Baker, R.A. Ghanem, Study on removal behavior and separation efficiency of naturally occurring bentonite for sulfate from water by continuous column and batch methods, Eur. J. Chem., 6 (2015) 12–20.

[9] H. Daraei, A. Mittal, M. Noorisepehr, F. Daraei, Kinetic and equilibrium studies of adsorptive removal of phenol onto eggshell waste, Environ. Sci. Pollut. Res., 20 (2013) 4603–4611.

[10] J. Wang, C. Chen, Biosorbents for heavy metals removal and their future, Biotechnol. Adv., 27 (2009) 195–226.

[11] P.V. Nidheesh, R. Gandhimathi, S.T. Ramesh, T.S.A. Singh, Adsorption and desorption characteristics of crystal violet in bottom ash column, J. Urban Environ. Eng., 6 (2012) 18–29.

[12] Z. Aksu, F. Gonen, Biosorption of phenol by immobilized activated sludge in a continuous packed bed: prediction of breakthrough curves, Process Biochem., 39 (2004) 599–613.

[13] T.V.N. Padmesh, K. Vijayaraghavan, G. Sekaran, M. Velan, Batch and column studies on biosorption of acid dyes on fresh water macro alga *Azolla filiculoides*, J. Hazard. Mater., 125 (2005) 121–129.

[14] D.C. Ko, J.F. Porter, G. McKay, Optimised correlations for the fixed-bed adsorption of metal ions on bone char, Chem. Eng. Sci., 55 (2000) 5819–5829.

[15] S. Samatya, N. Kabay, Ü. Yüksel, M. Arda, M. Yüksel, Removal of nitrate from aqueous solution by nitrate selective ion exchange resins, React. Funct. Polym., 66 (2006) 1206–1214.

[16] M. Jain, V.K. Garg, K. Kadirvelu, Cadmium(II) sorption and desorption in a fixed bed column using sunflower waste carbon calcium–alginate beads, Bioresour. Technol., 129 (2013) 242–248.

[17] H.C. Thomas, Heterogeneous ion exchange in a flowing system, J. Am. Chem. Soc., 66 (1944) 1664–1666.

[18] Y.H. Yoon, J.H. Nelson, Application of gas adsorption kinetics I. A theoretical model for respirator cartridge service life, Am. Ind. Hyg. Assoc. J., 45 (1984) 509–516.

[19] Annual Book of ASTM Standards D5029–98, Standard Test Method for Water-Soluble in Activated Carbon, 2002.

[20] Annual Book of ASTM Standards D2867–99, Standard Test Method for Moisture in Activated Carbon, 15 (2002) 801–803.

[21] A. Shahidi, N. Jalil Nejad Falizi, A. Jalil Nejad Falizi, Evaluation of the performance of Lufa natural adsorbent in the removal of divalent cadmium from aqueous medium, J. Water Wastewater, 3 (2015) 61–51.

[22] P. Sivakumar, P.N. Palanisamy, Adsorption studies of basic Red 29 by a non-conventional activated carbon prepared from *Euphorbia antiquorum* L, Int. J. Chem. Technol. Res., 1 (2009) 502–510.

[23] K. Baek, S. Song, S. Kang, Y. Rhee, C. Lee, B. Lee, S. Hudson, T. Hwang, Adsorption kinetics of boron by anion exchange resin in packed column bed, J. Ind. Eng. Chem., 13 (2007) 452–456.

[24] A.P. Lim, A.Z. Aris, Continuous fixed-bed column study and adsorption modeling: removal of cadmium(II) and lead(II) ions in aqueous solution by dead calcareous skeletons, Biochem. Eng. J., 87 (2014) 50–61.

[25] R.P. Han, Y. Wang, W.H. Zou, Y.F. Wang, J. Shi, Comparison of linear and nonlinear analysis in estimating the Thomas model parameters for methylene blue adsorption onto natural zeolite in fixed-bed column, J. Hazard. Mater., 145 (2007) 331–335.

[26] T.A.H. Nguyen, H.H. Ngo, W.S. Guo, T.Q. Pham, F.M. Li, T.V. Nguyen, X.T. Bui, Adsorption of phosphate from aqueous solutions and sewage using zirconium loaded okara (ZLO): fixed-bed column study, Sci. Total Environ., 523 (2015) 40–49.

[27] H.P. Chao, C.C. Chang, A. Nieva, Biosorption of heavy metals on *Citrus maxima* peel, passion fruit shell, and sugarcane bagasse in a fixed-bed column, J. Ind. Eng. Chem., 20 (2014) 3408–3414.